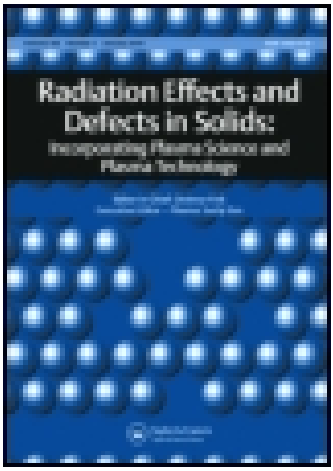

Radiation Effects and Defects in Solids: Incorporating Plasma Science and Plasma Technology
Publication details, including instructions for authors and subscription information:
http://www.tandfonline.com/loi/grad20

Computer simulation of high energy displacement cascades

H. L. Heinisch [a]

[a] Pacific Northwest Laboratory , P.O. Box 999, Richland, WA, 99352, USA

Published online: 13 Sep 2006.

To cite this article: H. L. Heinisch (1990) Computer simulation of high energy displacement cascades, Radiation Effects and Defects in Solids: Incorporating Plasma Science and Plasma Technology, 113:1-3, 53-73, DOI: 10.1080/10420159008213055

To link to this article: http://dx.doi.org/10.1080/10420159008213055

Radiation Effects and Defects in Solids, 1990, Vol. 113, pp. 53–73
Reprints available directly from the publisher
Photocopying permitted by license only

COMPUTER SIMULATION OF HIGH ENERGY DISPLACEMENT CASCADES

H. L. HEINISCH

Pacific Northwest Laboratory, P.O. Box 999, Richland, WA 99352 USA

Presented at the Workshop on Effects of Recoil Energy Spectrum and Nuclear Transmutations on the Evolution of Microstructure, March 24–29, 1988 at Lugano, Switzerland

A methodology developed for modeling many aspects of high energy displacement cascades with molecular level computer simulations is reviewed. The initial damage state is modeled in the binary collision approximation (using the MARLOWE computer code), and the subsequent disposition of the defects within a cascade is modeled with a Monte Carlo annealing simulation (the ALSOME code). There are few adjustable parameters, and none are set to physically unreasonable values. The basic configurations of the simulated high energy cascades in copper, i.e., the number, size and shape of damage regions, compare well with observations, as do the measured numbers of residual defects and the fractions of freely migrating defects. The success of these simulations is somewhat remarkable, given the relatively simple models of defects and their interactions that are employed. The reason for this success is that the behavior of the defects is very strongly influenced by their initial spatial distributions, which the binary collision approximation adequately models. The MARLOWE/ALSOME system, with input from molecular dynamics and experiments, provides a framework for investigating the influence of high energy cascades on microstructure evolution.

Key words: binary collision, copper, computer simulation, MARLOWE, ALSOME, cascades, subcascades, annealing, defect production, freely migrating defects.

1 INTRODUCTION

One of the greatest challenges in developing materials to withstand the neutron radiation in deuterium–tritium fusion reactors is having to proceed in the absence of a relevant fusion neutron environment. This has created a need for developing correlations so materials can be tested in other irradiation test facilities, primarily fission reactors. The basis of the correlation process lies in understanding the fundamental aspects of radiation effects, especially the energy dependence of radiation damage events. Because primary damage information is not easily accessible experimentally, quantitative results from primary damage modeling are valuable in developing the correlations, especially in the role of providing source terms for models of microstructure evolution.

Molecular level computer simulations of radiation damage events can give quantative information on the initial damage state, e.g., the energy dependence of the numbers of total defects, freely migrating defects, and clusters. More importantly, these simulations provide the most complete description of the initial spatial distribution of defects formed in cascades, which has a very strong impact on how the defects interact.

For about 25 years molecular dynamics has been used for modeling primary damage, but until recently, only very low energy events have been modeled. This method has suffered from two major shortcomings preventing its usefulness in simulating displacement cascades: the lack of realistic interatomic potentials and the need for great computer size and speed to model displacement cascades of sufficiently high energy to observe typical cascade effects. New approaches in which local electron densities are accounted for in a semi-empirical pair potential

formulation[1] appear to be a major breakthrough in realistic treatment of atomic interactions at a level of realism and computational complexity commensurate with molecular dynamics modeling of displacement cascades. The existence of large, fast vector computing machines should soon allow us to model displacement cascades that have sufficiently high energy to exhibit some of the cascade effects relevant to fission–fusion correlations.

The operational definition of "high energy" in computer simulations of displacement cascades is that energy above which the problem saturates the largest available computer, about 5 keV in the most recent molecular dynamics simulations.[2] With respect to damage correlation, "high energy" refers to the primary knock-on atom (PKA) energy above which most of the damage is produced in 14 MeV neutron irradiations. In typical structural alloys 90% of the point defects from 14 MeV neutrons are produced in cascades of 100 keV or greater. With respect to the physical processes being modeled, "high energy" might be defined as the PKA energy above which more than one distinct damage region is produced, about 20–50 keV. The break-up of high energy cascades into subcascades is well-established both theoretically[3] and experimentally.[4] The last definition of high energy will be used here.

The average energy of PKAs resulting from 14 MeV neutrons is about 200 keV in structural metals. While modeling a 200 keV cascade with molecular dynamics is well beyond the capabilities of present or even planned supercomputers, it is very probable that at least individual subcascades of high energy cascades can eventually be modeled with molecular dynamics. However, there are aspects of high energy cascades that can never be studied with molecular dynamics, such as the spatial distribution of subcascades and the long-term development of the defect interactions in the cascade. Binary collision models, which ignore many of the low energy details of atomic interactions, are excellently suited for describing the gross structural features of high energy cascades, and they will continue to be useful in the overall modeling scheme.

In this paper a methodology for modeling high energy cascades with the binary collision code MARLOWE and the Monte Carlo annealing code ALSOME will be reviewed. Limitations of the models will be discussed, as well as the successes in simulating experimentally observed phenomena. Future directions for simulation of high energy cascades will be discussed.

2 MODELING HIGH ENERGY CASCADES

2.1 *Stages of Cascade Development*

Several stages of development can be identified during the production of a displacement cascade. First is the collisional stage of about 10^{-13} s, ending approximately when no atom has enough energy to displace another atom from its lattice site. The cascade quenching stage then occurs. During the next 10^{-11} s, the region of the crystal that has been violently disturbed by the cascade approaches thermal equilibrium with its surroundings while the defects athermally rearrange themselves. The effects of quenching are assumed to be independent of the crystal temperature. There is evidence from recent molecular dynamics simulations that a molten condition exists initially in the core of a cascade,[2] and that it may lead to spontaneous formation of vacancy loops during quenching. Finally, during the short-term annealing stage, lasting another 10^{-8} s or longer, the defects within the

cascade interact among themselves through thermally activated processes determined by the local crystal temperature. The transitions from one stage to the next are obviously not distinct; however, within the simulation scheme, criteria are arbitrarily chosen to define the end of each stage, since different models are used to describe each stage.

2.2 *The MARLOWE Code*

A comprehensive study of high energy cascades in copper was done utilizing the binary collision code MARLOWE[5] and the Monte Carlo annealing simulation code ALSOME.[6] The methodology for modeling high energy cascades in copper was developed and laid out in a series of reports. First the link between molecular dynamics and the binary collision approach was established at low energies[7] and high energies.[8] Numbers of defects in MARLOWE-generated cascades were compared with measured values at 4 K.[9] The effects of including thermal displacements in MARLOWE were studied.[10] Cascade configurations—shape, size and subcascade structure—were systematically studied.[3, 10] The fast Monte Carlo annealing simulation code ALSOME was developed and used to model quenching and short-term annealing of the cascades.[6, 9] More than a thousand cascades, ranging in energy from 200 eV to 500 keV were simulated in copper[11] using MARLOWE with thermal displacements representative of 300 K and parameter settings as described in Table I. Finally, functions describing production of total defects and freely migrating defects as a function of pka energy were devised and used to generate neutron cross sections for defect production.[12] Throughout this work care was taken to match the model wherever possible to experimental measurements without introducing additional, artificial parameters.

TABLE I
MARLOWE parameter settings for cascades generated in copper at 300 K

Code version:	11
Interatomic potential:	Molière approximation to Thomas–Fermi, with screening length of 7.38 pm
Inelastic losses:	Local (Firsov)
Lattice parameter:	ALAT = 0.3615 nm
Maximum impact parameter:	RB = 0.62 lattice parameters
Debye temperature:	TDEBYE = 314 K
Energy criteria for displaced atoms:	EDISP = 5.0 eV EQUIT = 4.8 eV EBND = 0.2 eV

In using the binary collision approximation the ability to deal exactly with the many-body aspects of low energy collisions is sacrificed for the facility of dealing with high energy cascades. The cascade is generated in a series of two-body collisions between atoms that originally occupy lattice sites in the crystal. Target atoms are added to the cascade if they receive a minimum kinetic energy in a collision. All displaced atoms are required to surmount a binding energy, and they are followed until their energies fall below a cut-off energy. A lattice temperature is accounted for by imposing a random thermal displacement on each target atom from a Gaussian distribution of uncorrelated displacements in the Debye model.

The results are sensitive to whether or not thermal displacements are included, but they are not very sensitive to the value of the temperature.[6] Electronic energy losses were accounted for in our modeling by subtracting the appropriate energy at each collision in the Firsov model. Quantitative measures of the damage energy referred to in this paper are the average damage energies determined in the MARLOWE code. The MARLOWE values of damage energy are within a few percent of the damage energies calculated from Robinson's formula for the Lindhard theory.[13]

Although the binary collision approximation is valid only for high energy collisions, the MARLOWE code contains parametric representations of some kinematic phenomena that can be set to produce appropriate results at low energies. Robinson[7] investigated the low energy behavior of MARLOWE and determined parameter settings that gave a reasonable fit to the replacement sequence lengths in copper determined from molecular dynamics. Robinson also concluded that it is necessary to include thermal displacements in MARLOWE to give correct low energy behavior. The values of the MARLOWE parameter settings for correct kinematic behavior in low energy events in copper are given in Table I.

MARLOWE models only the collisional stage of the cascade and cannot model relaxation about defects or the dissipation of energy to the rest of the crystal. Thus, a "MARLOWE cascade" consists of a list of positions of vacant lattice sites (vacancies) and energetic displaced atoms (interstitials) "frozen" at the turning points of their last collisions. The approaches used to model the quenching and short-term annealing stages utilize the ALSOME code, and will be discussed later.

2.3 *Cascade Configurations*

Our objective in modeling displacement cascades was to determine the numbers of defects produced and their spatial distribution as a function of cascade energy, along with the evolution and interaction of the defect distributions as a function of time and temperature. The evolution is strongly dependent on the defect configuration produced during the collisional phase.[6]

The configurations of MARLOWE-generated cascades in copper were analyzed graphically.[3, 10] Indispensible qualitative information was obtained from three-dimensional plots of the positions of vacancies and interstitials that were rotated in three dimensions in real time on a screen. Graphical analysis of hard-copy plots and numerical analysis of defect distributions were also done to obtain quantitative results. Figure 1 shows 3-D plots of cascades with energies ranging from 1 keV to 100 keV.

Distinct subcascades (damage regions separated by relatively undamaged material) are produced regularly at 50 keV and above. At lower energies and within individual subcascades there are separate, distinct regions of high defect density, often in close proximity (Figure 1). Thus, a separate category of cascade sub-region, the "lobe," was defined as the basic unit of cascade configurations. (An L-shaped distribution, for example, would be considered to have two lobes.) A special category of subcascades was also defined: widely-separated subcascades, for which the edge-to-edge separation is at least as large as the subcascade dimensions.

The energy dependence of lobe production is illustrated in Figure 1. At PKA energies up to a few keV the cascades have no fully developed lobes, but consist of a few scattered defects with the vacancies generally in the center. As the energy

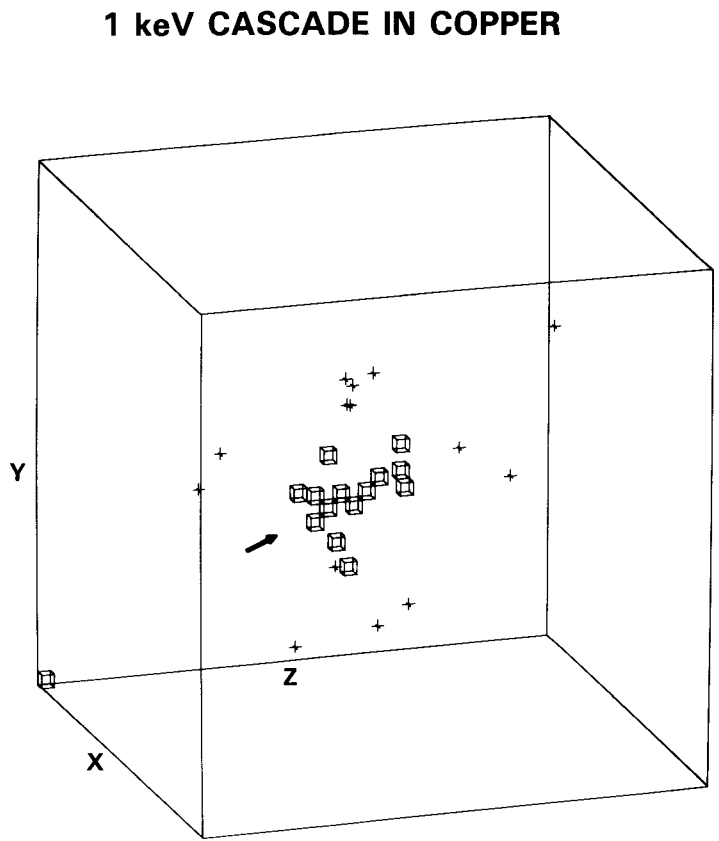

1(a)

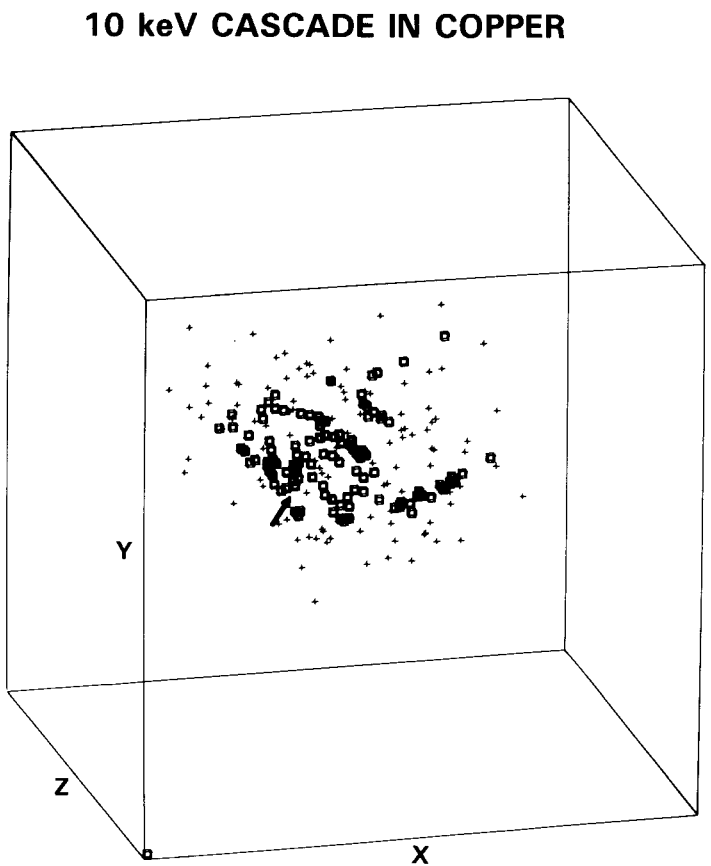

1(b)

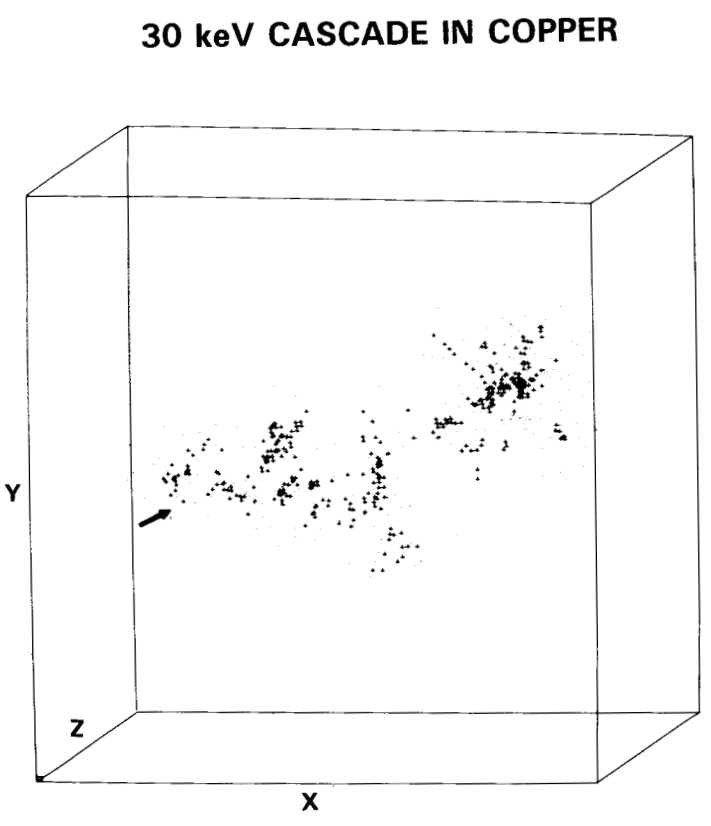

1(c)

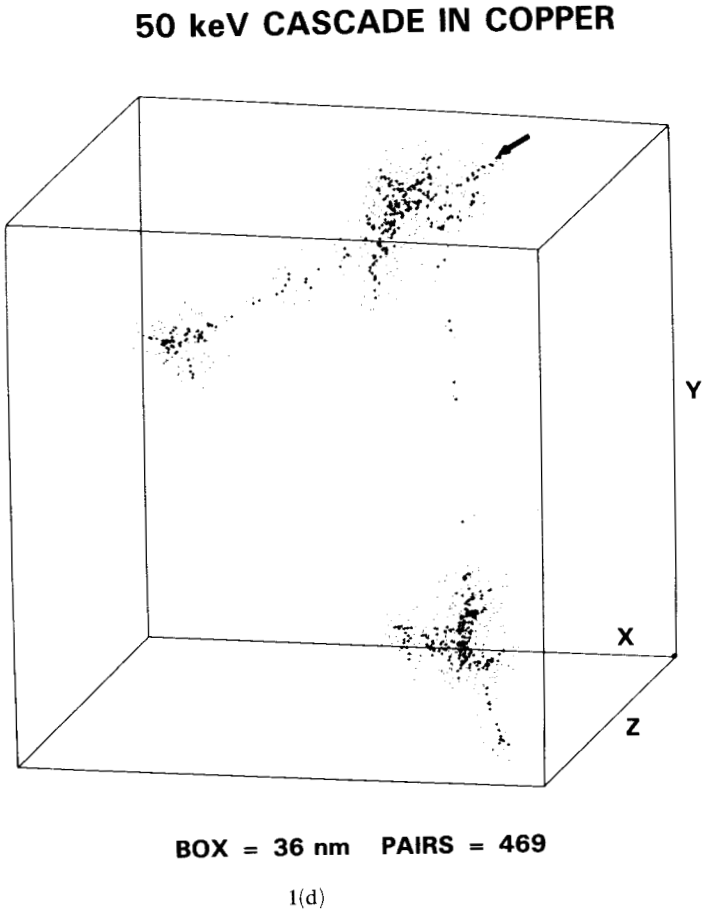

1(d)

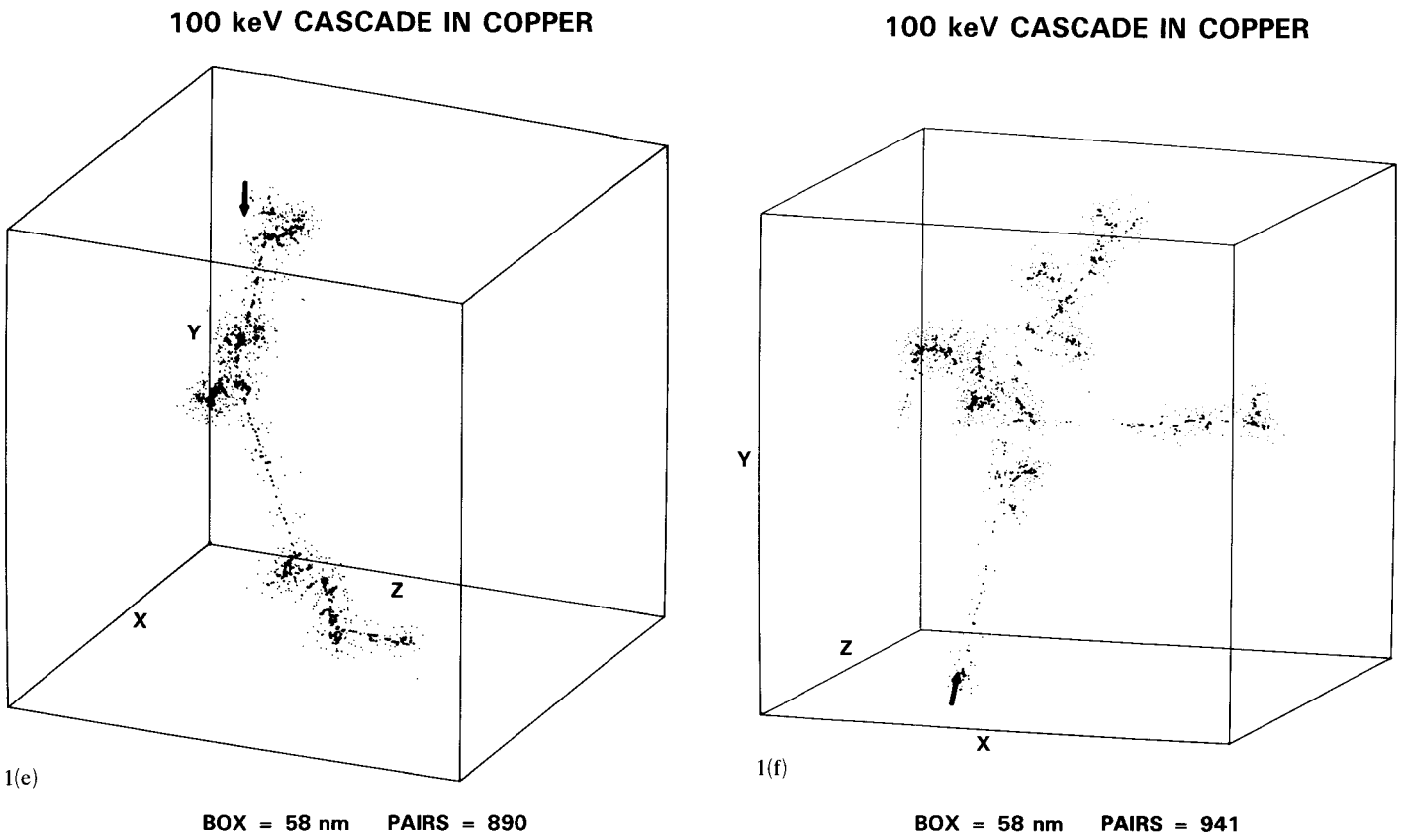

FIGURE 1 Three-dimensional views of cascades in copper at 300 K generated with MARLOWE. The small cubes represent vacancies and the pluses represent interstitials. A small arrow indicates the location and direction of the PKA. The cascades were subjected to a recombination radius of 2 lattice parameters, yielding numbers of defects equal to that calculated by the modified Kinchin and Pease expression.

increases (to about 10 keV in copper), single lobes become fully developed, with the characteristic vacancy-rich depleted zone surrounded by a cloud of interstitials. By about 20 keV the tendency to form more than one depleted zone or lobe is observed. And by 100 keV, widely-spaced subcascades, each having its own lobe structure, occur regularly.

Sizes of our simulated cascades and the numbers, size and spacing of lobes were determined as a function of PKA energy and damage energy.[10, 11] For the purpose of quantitative analysis, the minimum sized lobe was defined such that all 20 keV cascades have at least one lobe. Based on the present sample of cascades, extremely separated damage regions (with subcascade separations exceeding 2 or 3 times the average maximum extent for cascades of that energy) occur in less than 20% of cascades of 200 keV or less, and only rarely below 50 keV. Thus, for most of the PKAs produced in copper by 14 MeV neutrons, subcascades from the same PKA should be clearly associated with each other.

In brief, a high energy cascade in copper was found to be a series of mostly-connected 5 to 30 keV lobes separated by an average center-to-center spacing of 14 nm (including distances between widely-separated subcascades). On average there is approximately one lobe per 13 keV of damage energy. The numbers of lobes and distinct subcascades as a function of PKA damage energy are shown in Figure 2.

In recent transmission electron microscopy (TEM) investigations of pure metals irradiated by 14 MeV neutrons, Kiritani[14] was able to resolve individual sub-regions of single cascades. The numbers of sub-regions and their spacings are consistent with the lobe structures of our simulated cascades. Kiritani reports an inter-lobe spacing of 12 nm for copper, in good agreement with our simulations.

The technique of imaging disordered regions caused by cascades in ordered alloys[15] can give quantitative information on cascade shapes and sizes even when the residual defects cannot be imaged. The transverse dimensions of disordered regions produced by 10–200 keV Cu^+ ions normally incident on ordered Cu_3Au were analyzed by Jenkins *et al.*[16] Closely spaced multiple damage regions were observed. Maximum zone size distributions were determined, and the average maximum transverse dimensions were determined as a function of energy.

A simulation of this experiment was performed using MARLOWE[17] The sizes of the simulated point defect distributions were calibrated to the measured size distributions of disordered zones at 10 and 30 keV. A comparison of the simulated and experimental cascade dimensions is in Figure 3. To account for the foil thickness used in the experiment, the simulated cascade damage residing in only the first 20 nm of the foil was analyzed. The agreement between the simulation for the thin foil and the experiment was quite good over the entire energy range.

2.4 *Defect Densities*

Because high energy cascades are so irregular in shape, it is very difficult to make meaningful quantitative descriptions of their sizes or, especially, the density of defects. How one defines the density or volume depends largely on the use to be made of the information. In the narrowest definition of cascade volume, Robinson[18] multiplies the atomic volume by the number of moving atoms in a MARLOWE cascade. The defect density remains constant with damage energy by that definition of volume. At the other extreme, we have measured the volume inside a rectangular parallelepiped just enclosing the cascade.[11] Using that definition of volume, defect densities decrease with increasing energy by several orders of magnitude from

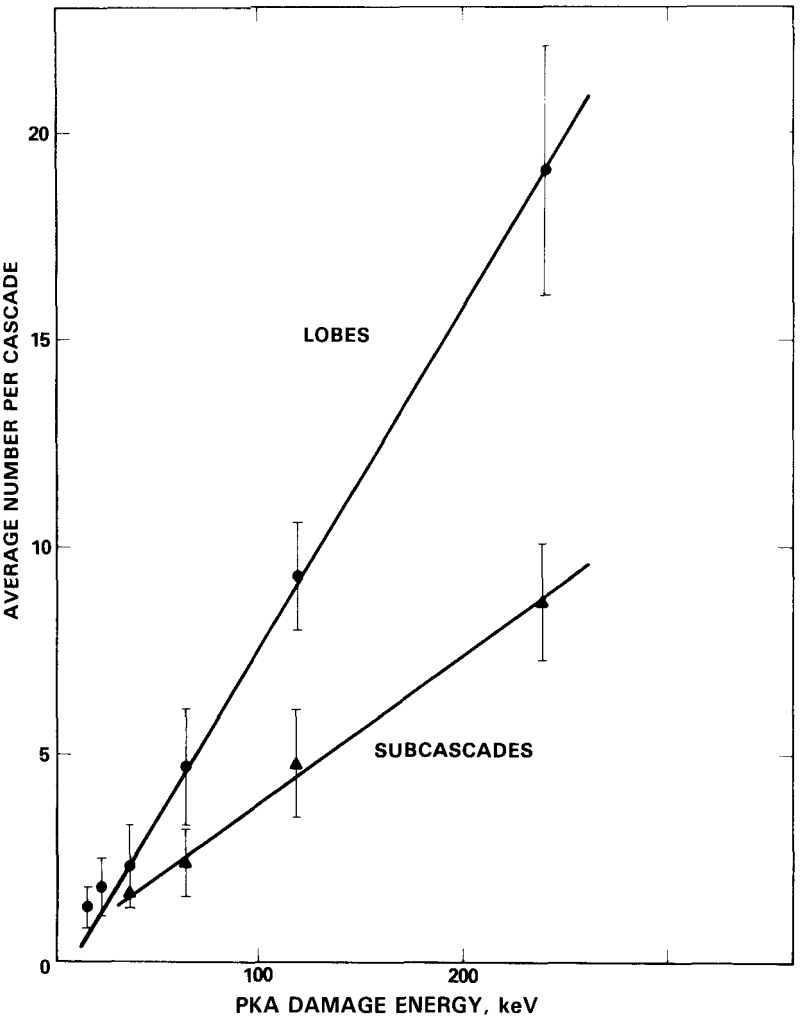

FIGURE 2 Average number of lobes and widely-spaced subcascades as a function of PKA damage energy, T_D, in keV.

1-200 keV. Figure 4 is a plot of the average defect density within the parallelepiped as a function of PKA energy. The data display a different energy dependence above about 20 keV, indicating the transition to multiple lobe production.

Volume determinations deriving from statistics of the defect distribution have been developed. They are best suited to single lobed cascades. The component analysis of ellipsoids was applied by Hou[19] to MARLOWE cascades up to 30 keV in tungsten. Dierckx[20] applied component analysis to individual subcascades in high energy cascades in alpha-iron. Benedek[21] analyzed cascades in copper using the radius of gyration of the defect distribution. The densities are proportional to the enclosing parallelepiped densities shown in Figure 4.

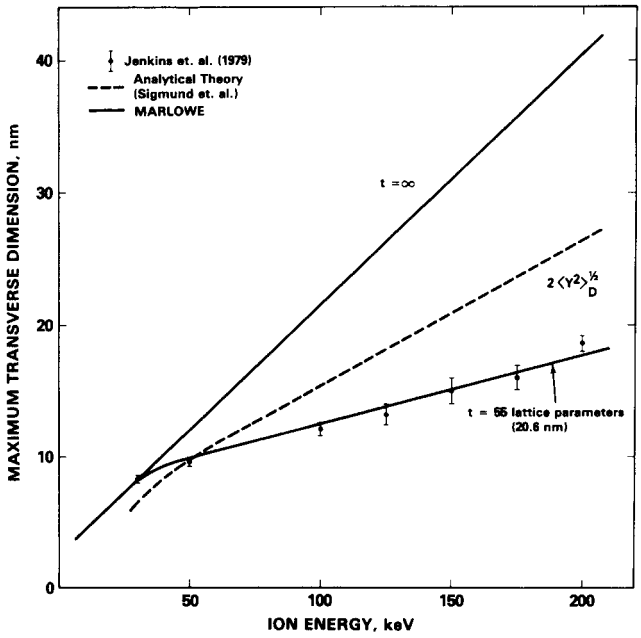

FIGURE 3 The measured maximum transverse dimension of disordered zones in ordered Cu_3Au irradiated with Cu^+ ions (points). The solid curves are results of MARLOWE simulations for thick ($t = \infty$) and thin ($t = 20.6$ nm) foils. The dashed line is the result of an analytical theory.

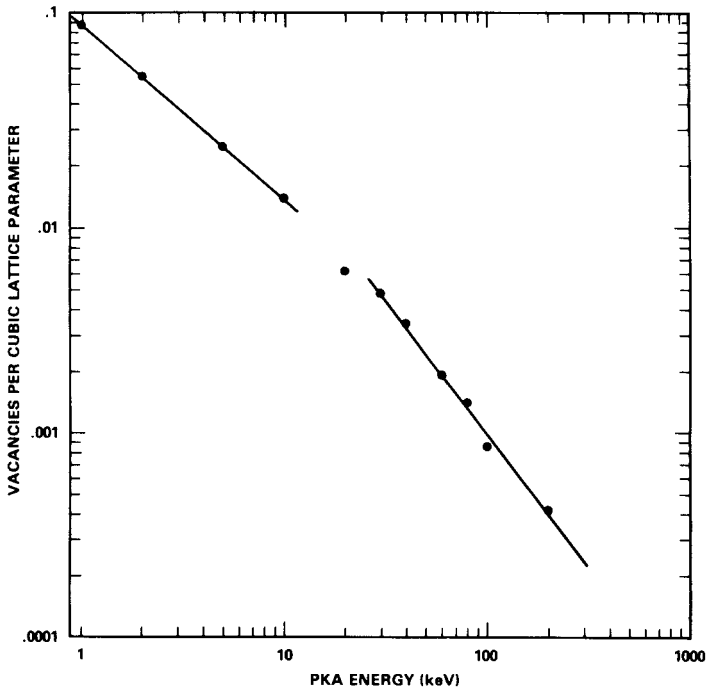

FIGURE 4 The average density of defects within the enclosing rectangular parallelepiped, oriented along the crystal axes, as a function of PKA energy.

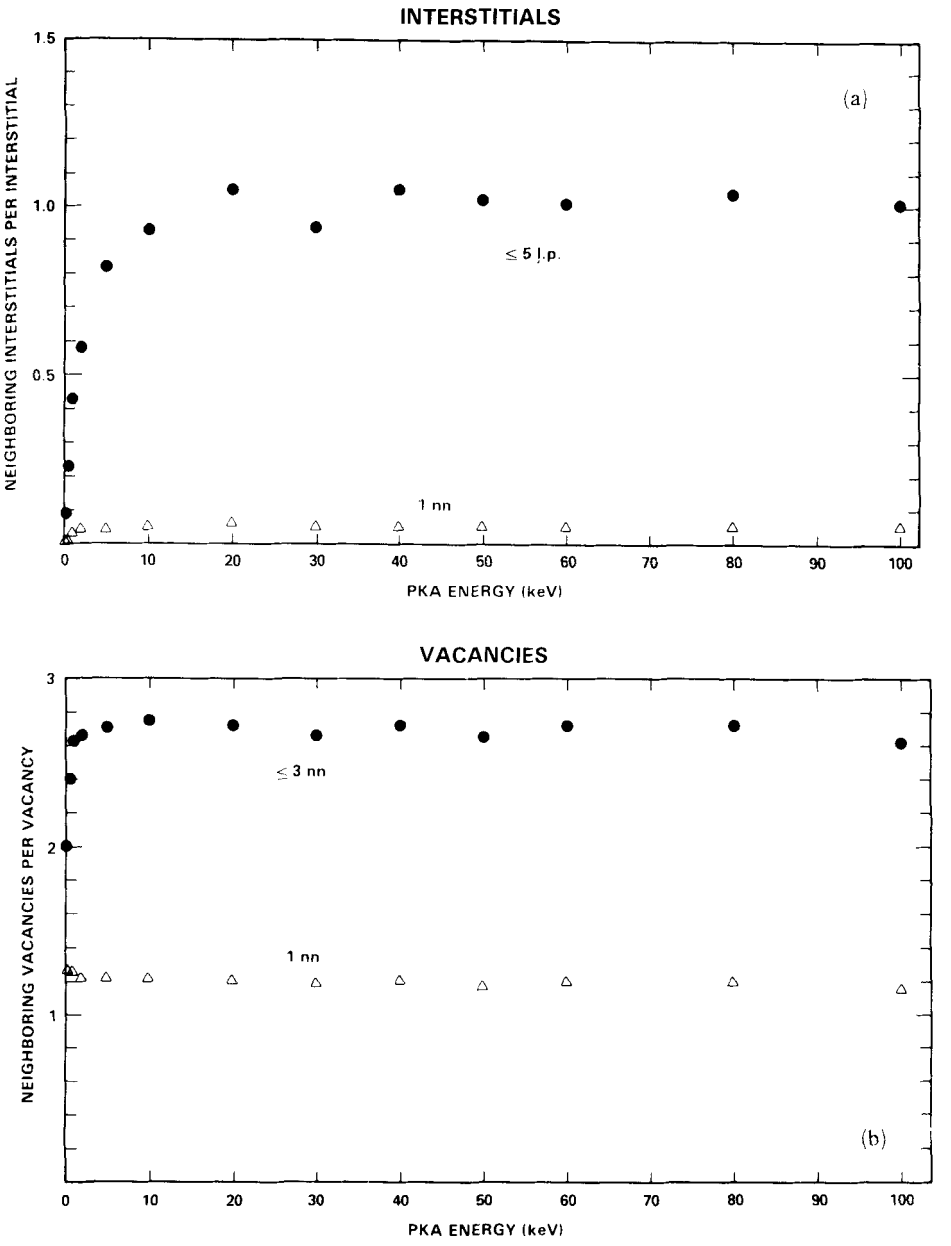

FIGURE 5 Average local density of (a) interstitials and (b) vacancies as a function of PKA energy, defined as the average number of neighboring defects within 5 lattice parameters (≤ 5 l.p.) for interstitials or 3 nearest neighbors (≤ 3 nn), 1.2 lattice parameters, for vacancies. The average number of nearest neighbor defects is also shown (1 nn) for each defect type.

In Figure 5 the average defect density in a small region about each defect is plotted as a function of PKA energy for vacancies and interstitials. Above about 10 keV, the defects see the same average environment, independent of energy. The subsequent behavior of the defects will initially be most influenced by their

immediate surroundings, thus, one can expect to learn much about high energy cascades by studying the evolution of individual lobes.

2.5 *Channeling*

The production of subcascades is, in general, a manifestation of the increase in the mean free path between energetic collisions with increasing energy of the projectile atom. Another phenomenon that may have an influence on the configurations of cascades is planar channeling. It occurs when an energetic primary or secondary knock-on atom is given a trajectory between two atomic planes such that relatively low energy collisions tend to confine the trajectory to that plane over a fairly large distance with only a small loss of projectile energy. Upon de-channeling, the projectile can produce a damage region widely separated from the rest of the cascade.

Computer simulations[11] indicate that channeling occurs in copper, though rarely, in cascades of 30 keV or less. In these lower energy cascades the appearance of channeling is quite dramatic, since in the absence of channeling, usually only a single, compact damage region is produced. In cascades with hundreds of keV of energy, subcascades are produced in locations that may or may not be the result of channeling. MARLOWE cascades of 200 and 500 keV in copper were analyzed graphically to determine the contribution of channeling to the cascade configuration. The trajectory directions for 74 events in 40 cascades were determined from debris along the trajectory (an occasional Frenkel pair) or inferred from relative shapes and positions of damage regions, Figure 6a. Of the events measured, 68% have directions within 2° of a planar channeling direction. If directions were randomly chosen, about 41% of all directions would be in this category. Thus, it seems that channeling events occur frequently in high energy cascades in copper, but they are not the exclusive mechanism by which widely separated damage regions are produced.

The influence of channeling events on the configurations of high energy cascades was also investigated by comparing simulated cascades produced in crystalline and "amorphous" copper. MARLOWE models an amorphous material by performing a random rotation of the lattice after each collision. While this procedure does not rigorously represent the amorphous condition, nevertheless, the symmetry that permits channeling is destroyed. A comparison of the vacancy distributions of 200 keV cascades in crystalline and amorphous copper showed that the cascades in crystalline material were only slightly larger in extent and aspect ratio. The amorphous cascades, Figure 6b, are generally indistinguishable from the crystalline cascades, but on the average, they tend to have fewer widely-separated damage regions. In real situations if the opportunity for channeling is suppressed, the subsequent interactions of the defects may be affected. Additionally, conditions that suppress channeling would probably also suppress replacement collision sequences, which would have an even greater impact on subsequent defect interactions.

2.6 *Cascade Quenching and Short-term Annealing*

The quenching stage of a high energy cascade can only be properly simulated by a fully dynamical model, a feat that has yet to be achieved above 5 keV in copper. The binary collision approach is inadequate for modeling the many body aspects of the quenching stage. Although it can model well the gross features developed

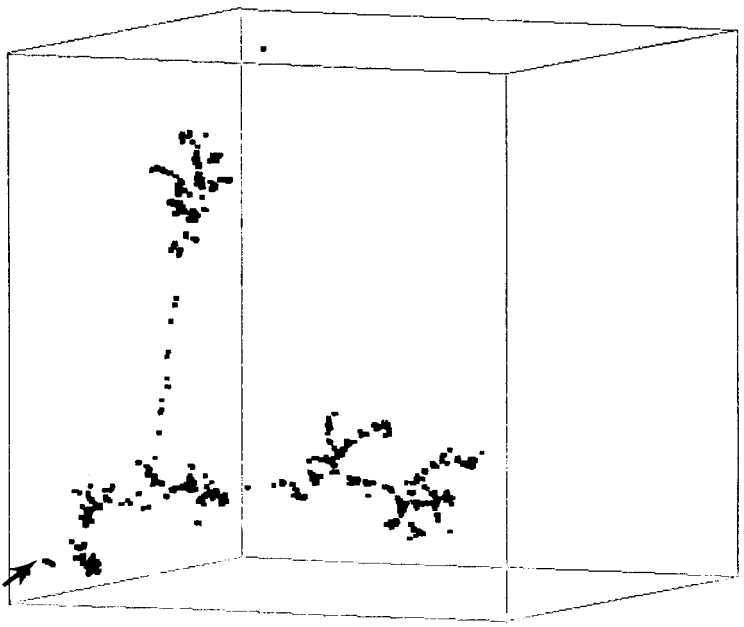

(a)

200 keV, BOX = 62 nm

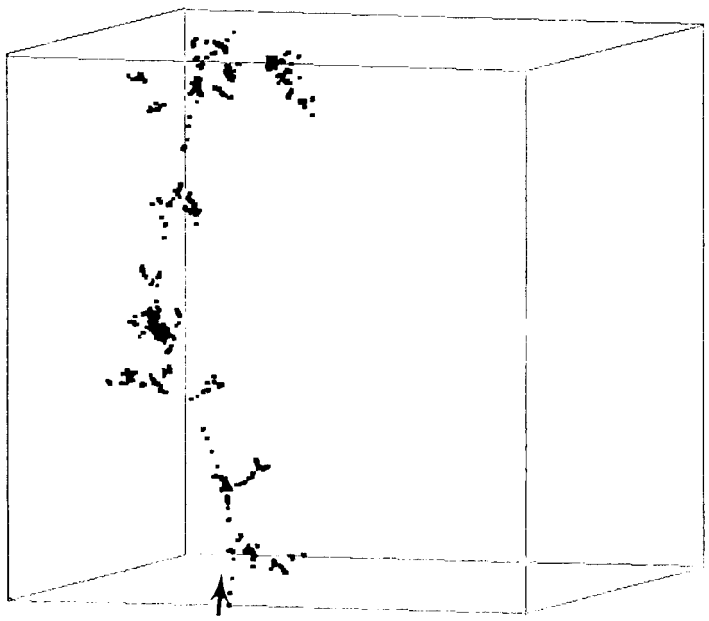

(b)

"AMORPHOUS COPPER"
200 keV, BOX = 69 nm

FIGURE 6 (a) Vacancy distribution for a 200 keV cascade in copper. The cube edge is 170 lattice parameters (62 nm). The vertical trail of single vacancies indicates the trajectory of the energetic recoil that produced the upper subcascade. (b) Vacancy distribution for a 200 keV cascade in "amorphous" copper. The cube edge is 192 lattice parameters (70 nm).

during the collisional stage, it does not leave the defects or the surrounding crystal in the correct disposition. However, it may be possible that a simple parametric model of cascade quenching, applied to MARLOWE cascades, can bridge the gap in a physically reasonable way between the collisional stage and the beginning of the short-term annealing stage. The major physical effects of quenching are significant recombination, clustering and, in some cases, direct formation of vacancy loops. As quenching is independent of crystal temperature, the number of defects remaining immediately after quenching at any temperature is assumed equal to that measured in irradiations at liquid helium temperature (approx. 4 K) where defects are immobile. Analyses[22-24] of experimental information show the recoil energy dependence of defect production. It is generally accepted that the lower efficiency of defect production in cascades is a result of recombination during quenching.

The simplest approach to representing the result of quenching in MARLOWE cascades is to ignore the kinetic and potential energy of the defects at the termination of the collisional stage and to statically recombine the closest defect pairs, leaving the residual defects in the positions determined by MARLOWE. In the earliest work,[9] a single, energy-independent recombination distance was found to give defect pair yields for cascades from 10 keV to 500 keV in copper equal to the measured number of defect pairs extracted[22] from resistivity measurements on copper irradiated with charged particles and neutrons at 4 K. The post-quenching number of defects was correct, but the spatial distribution of the residual defects was quite incorrect. About 25% of vacancies and 50% of interstitials became freely migrating defects during subsequent short-term annealing simulations of the recombined cascades. Experimental evidence (reviewed in Ref. 25) indicates that only a few percent of the defects that exist in the post-quenching primary damage state escape their cascades and become freely migrating defects.

As a first step toward a more realistic quenching model, a semi-empirical kinetic quenching model was devised within the framework of the short-term annealing simulation code ALSOME.[6] When applied to MARLOWE cascades of 1–100 keV in copper, both the observed numbers of total defects and the fractions of freely migrating defects (those that escape interactions within their own cascade) were well-modeled throughout the energy range.

2.7 *The ALSOME Code*

The Monte Carlo annealing simulation code ALSOME[6] contains a number of simplifying assumptions about the physical processes that make it very fast even for the largest cascades. (ALSOME is not presently available for distribution). Defect clusters are spherical and centered on lattice sites. Mobile defects are jumped in random sequence, weighted by their relative jump probabilities. When two defects come within a critical reaction distance, they are coalesced into a single defect. The only adjustable parameters in ALSOME are the relative jump probabilities of mobile defects and the critical reaction distances between various defect species. In practice, time is measured in terms of defect jumps and the concept of temperature enters when the sequence of events is interrupted. For example, if the simulation is terminated when few mobile interstitials remain, but before vacancies have started moving, the result represents the short-term annealing at a temperature where interstitials are relatively mobile and vacancies are relatively immobile. The real time at temperature is reflected in the absolute jump frequencies: the simulated real elapsed time is the inverse of the sum of the jump frequencies of the jumping

defects for the temperature being simulated. The results with ALSOME were found to be statistically indistinguishable[9] from simulations done with a more physically rigorous approach.[26]

For isolated cascades in copper, the sequence of simulated annealing events is fairly insensitive to the relative jump frequencies. Indeed, in an extreme test, little difference was found when vacancies were allowed to move before interstitials. This is a further manifestation of the strong effect of the initial defect configuration on subsequent behavior.

The kinetic quenching model consists of annealing cascades with ALSOME for a very short time with exaggerated parameter values. The quenching lasts for 100 interstitial jumps, about 10^{-11} s, which is consistent with arguments based on thermal conduction.[27] Cascades are taken from MARLOWE to ALSOME with no prior recombination. They are quenched with quenching values of ALSOME parameters, then short-term annealed with the conventional parameter settings.

2.8 *Freely Migrating Defects*

The numbers of defects remaining immediately after the quench compare very well with the defect yields extracted from resistivity measurements at 4 K, Figure 7. Then, after short-term annealing at approximately 300 K, the fractions of free defects compare well with measured values, 14% of the remaining interstitials[28] and

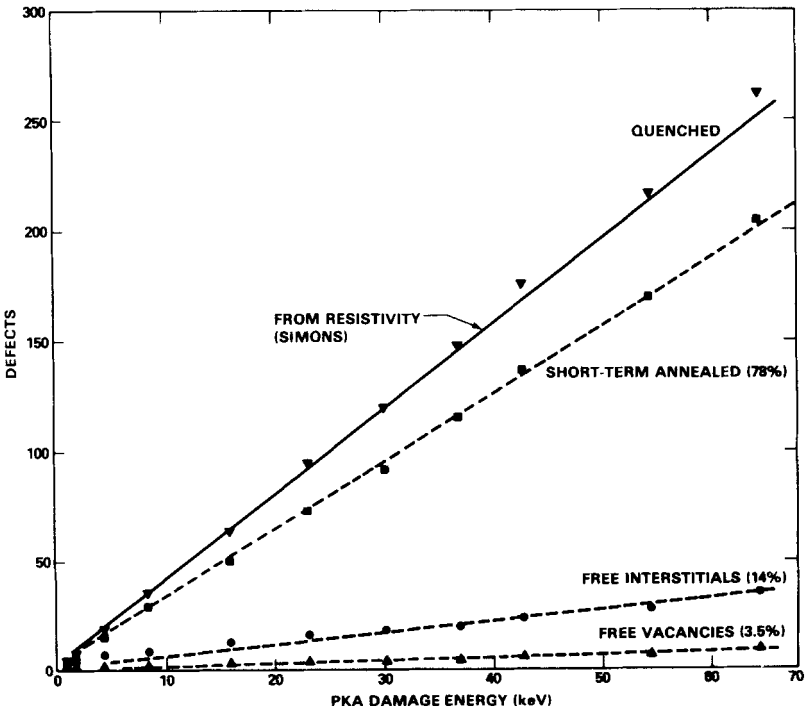

FIGURE 7 The number of defect pairs remaining after quenching and short-term annealing of isolated cascades in copper as a function of PKA damage energy. Free vacancies and interstitials are the defects that do not recombine or cluster within the cascade during annealing.

3.5% of remaining vacancies.[29] The defects that do not escape the cascade region remain simply as immobile clusters. The quenching model does not include provision for loop formation. However, during quenching, vacancy clusters were given radii representative of loops rather than spherical clusters, making large clusters more effective as sinks.

The fractions of free defects are sensitive to the critical reaction distances used, but their spatial distribution places bounds on their behavior. Regardless of the parameter settings, a minimum of 10% of the interstitials escape, because they are at the periphery of the cascade. A maximum of 10% of the vacancies can escape because of their concentration in the center of the cascade.

The energy dependence of free defect production at low energies is more specifically illustrated in Figure 8. The efficiency of total stable defect production measured at 4 K[22] relative to the displacements calculated from the modified Kinchin and Pease expression[30] is plotted as a function of PKA energy in Figure 8a. The fractions of total stable defects that become freely migrating defects after short-term annealing at 300 K are plotted in Figure 8b.

The higher efficiencies of total and free defect production at lower recoil energies are a manifestation of the energy dependence of lobe production, but in different ways. The energy dependence of the efficiency of total defect production is related to the density of defects in a cascade. Below about 1 keV there are few defect pairs created in close proximity, and the energy density of the cascade region is not great enough to cause recombination by quenching. With increasing energy, the density of defects and energy in the cascade volume increases, and recombination and clustering occur during quenching. The critical density for maximum quenching recombination (perhaps the critical energy density for formation of a molten phase[2]) is achieved by about 5 keV. As the energy increases further, the damage regions become larger, but the defect densities remain constant, as illustrated in the behavior of the average local densities of defects in Figure 5. The production of lobes and subcascades guarantees constant efficiency with further increase in energy.

The fractions of freely migrating defects are influenced by the surface areas of the vacancy core and the interstitial cloud making up the cascade. As the cascades increase in size with energy, the free defect fractions, which depend on the surface-to-volume ratios, decrease until the maximum lobe size is achieved, after which they remain constant as the increasing energy simply results in more lobes. The effect is greatest for the interstitials, which lie at the outer edge of the cascade region.

Correlations of property changes that depend on total defect production by neutrons from fission and fusion reactors should not be affected much by the recoil energy dependence of total defect production efficiency. In most fission reactors the vast majority of displacements result from recoils above 1 keV. However, property changes that depend on freely migrating defects at room temperature may show significant neutron spectral effects. Functions fitted to the simulation results for free defects[12] have been folded into PKA spectra for 14 MeV neutrons and the Fast Flux Test Facility (FFTF) at Hanford, Washington. The calculations predict that, compared to 14 MeV neutrons, FFTF produces twice as many free interstitials and three times as many free vacancies per DPA (displacements per atom), while producing the same number of total residual defects per DPA.

Recent experiments[25] measuring radiation induced segregation in ion bombarded Ni–Si and Cu–Au alloys at temperatures of 650–900 K, where clusters are unstable, show weighted recoil energy dependence of free defect production very

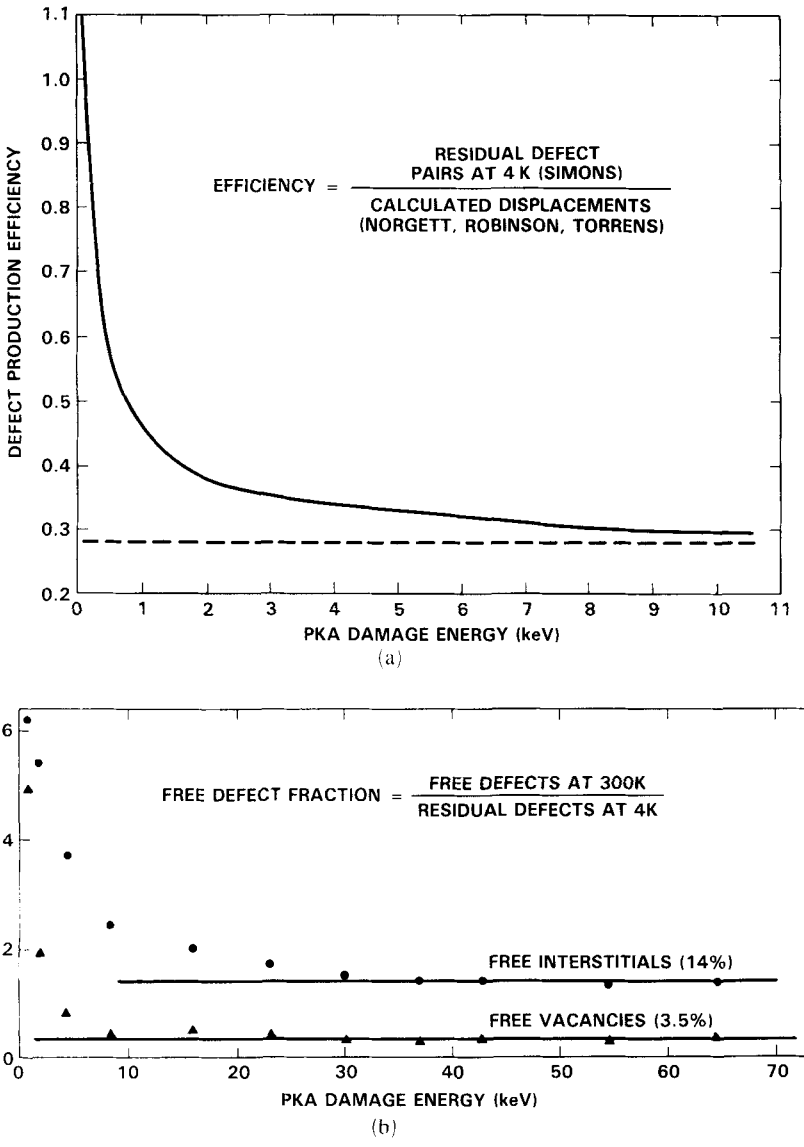

FIGURE 8 (a) PKA pair production efficiency for copper. Efficiency is the ratio of the residual defect pairs at 4 K, extracted from resistivity measurements (Simons), to the displacements calculated with the modified Kinchin and Pease expression (NRT). (b) The fractions of residual defects at 4 K that become freely migrating vacancies and interstitials after short-term annealing at 300 K.

similar to the modeling results in Figure 8b. This is evidence that even at high temperatures the initial cascade configuration also strongly influences the behavior of defects in cascades. The basic cascade configuration just after the collisional phase, i.e., vacancies surrounded by a cloud of interstitials, is essentially independent of temperature. Evidently, this configuration results in subsequent intense recombination within each cascade at high crystal temperatures. As at lower temperatures, the fraction of freely migrating defects is controlled by the

decreasing surface-to-volume ratio as cascade energy and size increase, leveling off as multiple lobe production begins at about 20–30 keV. This interpretation should be investigated by doing a short-term annealing simulation of cascades at high temperatures. The behavior implied by these experiments may lead to a considerable effect of the neutron spectrum on swelling and irradiation creep.

2.9 *Cascade Interactions*

The simulations discussed so far have been for single, isolated cascades. Phenomena of interest, and most experiments, take place with at least the possibility of cascade interactions. ALSOME simulations of cascade interactions have been done[6] and the results imply that the configuration of the initial damage state is a dominating influence. The free interstitials interact almost exclusively with other interstitials, clustering either with the free interstitials from other cascades or with interstitial clusters at the periphery of another cascade. Figure 9 shows interstitial and vacancy cluster size distributions for isolated and interacting 30 keV MARLOWE cascades in copper after annealing at 50 K (Stage I recovery) with ALSOME. For cascades allowed to interact during annealing there are more and larger interstitial clusters, while the vacancy clustering is the same. Stage I recovery of 18% was experienced by both the interacting and isolated cascades, compared to

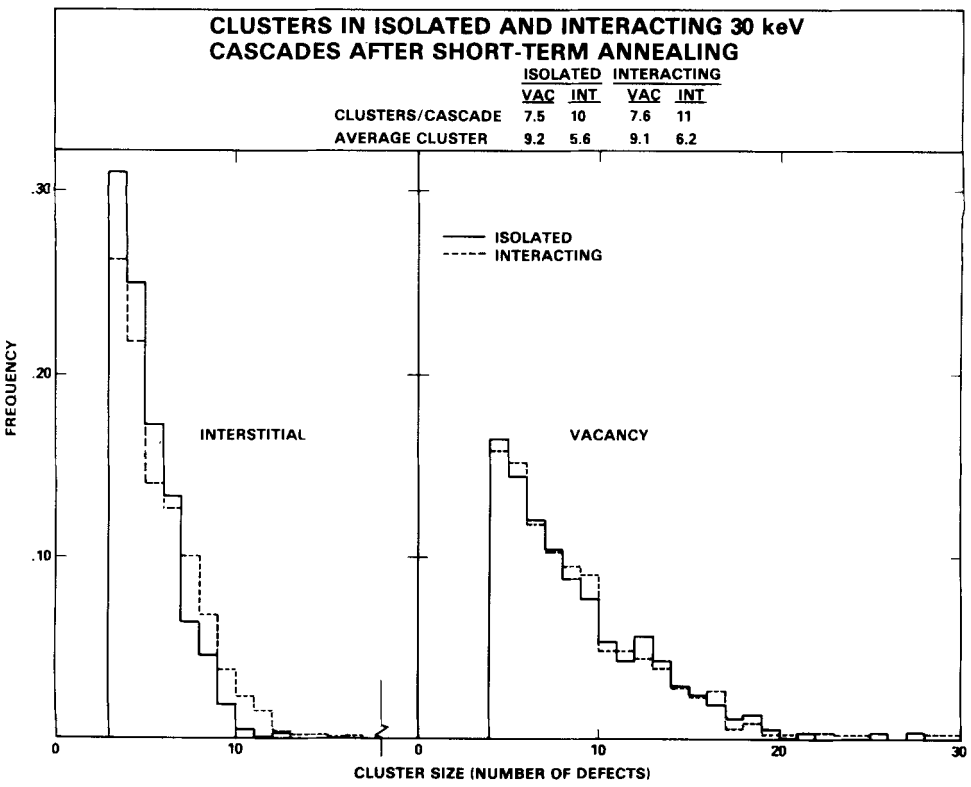

FIGURE 9 Cluster size distributions of isolated and interacting 30 keV cascades in copper after short-term annealing at 300 K.

80% for electron irradiation[31] and 35% for d-Be neutron irradiations.[32] The small amount of recovery in the simulation must be due, at least in part, to using 30 keV cascades exclusively. Simulations of specific annealing experiments should be done using a distribution of cascade energies representative of the recoil spectrum being simulated.

3 DISCUSSION

3.1 *Other High Energy Cascade Modeling*

Earlier simulations of high energy cascades by Doran and coworkers[26, 33, 34] included short-term annealing simulations and the determination of defect production functions. They used cascades generated in the pioneering simulation studies of Beeler.[35] Later cascades were generated in copper with an early version of MARLOWE. They annealed the cascades using a model somewhat more physically realistic than in ALSOME. the cut-off energy EQUIT used in MARLOWE was 25 keV, and no provision was made for recombination or clustering due to quenching. With the higher value of EQUIT, long replacement sequences were not allowed, and the average pair separation was too small; hence, more recombination would be expected during short-term annealing. However, since the effects of quenching were not taken into effect, the initial number of defects was too large in the annealing simulation. These factors apparently offset each other, because the residual defect production was very similar to that in Figure 7. While the total number of defects was fortuitously correct, the defects were not in the correct initial configuration: the post-annealing fractions of mobile defects were much too large.

Muroga and Ishino[36] have done binary collision simulations of high energy cascades in alpha-iron, along with short-term annealing simulations. With a high value of EQUIT (40 eV) and apparently no provision for quenching, their results are similar to those of Doran *et al.* Total residual defect production is correct, but the free defect fractions are very large compared to measured values (in fcc metals). Muroga *et al.*[37] have determined the recoil energy dependence of free defect fractions in simulated cascades from 30 eV to 30 keV. While these fractions are still very high compared to measured values, the overall energy dependence is similar to that obtained in our simulations for copper, Figure 8.

Dierckx[20] has generated cascades for PKAs from 500 eV to 2 MeV in alpha-iron with MARLOWE, using a fairly high value of EQUIT (25 eV). The general configurations of the cascades should be independent of the value of EQUIT used in various simulations. The cascade configurations were analyzed using a cluster identification algorithm, then each subcascade identified was treated by ellipsoid component analysis. The cluster algorithm cannot interpret the lobe structure of subcascades, so Dierckx's conclusions about the energy dependence of cascade configurations are somewhat different from ours. The subcascades are reported to become larger and less dense with increasing damage energy throughout the energy range.

3.2 *Future High Energy Cascade Modeling*

The major conclusion to be drawn from these simulations of high energy displacement cascades is that the initial defect configuration strongly influences the

subsequent behavior of the defects. The entire simulation scheme from cascade production through short-term annealing is accomplished with very simple models, based on fundamental actions of interacting particles. There are few adjustable parameters, and no unphysical parameter values are needed to produce good agreement with experimental results. So strong is the influence of the spatial distribution of defects, that some aspects of the annealing simulation are nearly insensitive to some parameter values. However, it should be noted that the conclusions stated here for copper may not all apply in other systems. For example, in materials having more diffuse cascades, the influence of the initial configuration on the final disposition of the defects may not be as strong.

As with all modeling, one must keep the results in proper perspective. The detailed characteristics of individual defects and their interactions can never be modeled correctly with MARLOWE and ALSOME, but many effects governed by large-scale spatial relationships can be modeled with sufficient accuracy to provide important and unique insights.

Computer codes such as MARLOWE and ALSOME should be used as a framework for investigating the influence of high energy cascades on microstructure evolution. The consequences of the detailed interactions can be determined with sufficient rigor elsewhere, most likely by molecular dynamics or direct experimental observation, and represented by simple models within a MARLOWE/ALSOME framework. Molecular dynamics simulations of critical sized lobes and loop formation in cascades are crucial to starting with the most realistic defect distributions. Careful, innovative experimental investigations of the primary damage state must continue to be done. Properly calibrated and parameterized for the problem under investigation, ALSOME can provide a realistic representation of many aspects of microstructure evolution because it incorporates the explicit spatial dependence necessary to study cascade effects.

ACKNOWLEDGEMENT

This work was supported by the U.S. Department of Energy under Contract DE-AC-76RLO 1830.

REFERENCES

1. M. S. Daw and M. I. Baskes, *Phys. Rev. B* **29,** 6443 (1984).
2. T. Diaz de la Rubia, R. S. Averback, and R. Benedek, *J. Mater. Res.* in press. See also contribution to this conference.
3. H. L. Heinisch, *J. Nucl. Mater.* **103/104,** 1325 (1981).
4. M. Kiritani, *J. Nucl. Mater.* **133/134,** 85 (1985).
5. M. T. Robinson and I. M. Torrens, *Phys. Rev. B* **9,** 5008 (1974).
6. H. L. Heinisch, *J. Nucl. Mater.* **117,** 46 (1983).
7. M. T. Robinson, *DAFS Quarterly Progress Report, January-March* 1980, DOE/ET-0065/9, U.S. Department of Energy, 54 (1980).
8. H. L. Heinisch, J. O. Schiffgens, and D. M. Schwartz, *J. Nucl. Mater.* **85/86,** 607 (1979).
9. H. L. Heinisch, D. G. Doran and D. M. Schwartz, *Effects of Radiation on Materials,* ASTM Special Technical Publication 725 191 (1981).
10. H. L. Heinisch, *J. Nucl. Mater.* **108/109,** 62 (1982).
11. H. L. Heinisch, *Computer Simulation of Displacement Cascades in Copper,* HEDL-TME 83-17 (1983).
12. H. L. Heinisch and F. M. Mann, *J. Nucl. Mater.* **122/123,** 1023 (1984).
13. M. T. Robinson, *Nuclear Fusion Reactors,* Proc. of the British Nuclear Energy Soc., UKAEA,
14. M. Kiritani, *J. Nucl. Mater.* **155-157,** 113 (1988).
Reactor Materials, Karlsruhe, Germany, Oct. 4–8, 1987 (1988).
15. M. L. Jenkins, K. H. Katerbau, and M. Wilkens, *Phil. Mag.* **34,** 1141 (1976).

16. M. L. Jenkins, N. G. Norton, and C. A. English, *Phil. Mag. A* **40,** 131 (1979).
17. H. L. Heinisch, *Phil. Mag. A* **45,** 1085 (1982).
18. M. T. Robinson, *Phys. Rev. B* **27,** 5347 (1983).
19. M. Hou, *Phys. Rev. B* **31,** 4178 (1985).
20. R. Dierckx, *J. Nucl. Mater.* **144,** 214 (1987).
21. R. Benedek, *J. Appl. Phys.* **52,** 5557 (1981).
22. R. L. Simons, *J. Nucl. Mater.* **141¢143,** 665 (1986).
23. P. Jung *et al.*, *ASTM STP* 782, eds. H. R. Brager and L. S. Perrin, 963 (1982).
24. J. H. Kinney, M. W. Guinan, and Z. A. Munir, *J. Nucl. Mater.* **122/123,** 1028 (1984).
25. L. E. Rehn and P. R. Okamoto, *Mater. Sci. Forum,* **15¢18,** 985 (1987).
26. D. G. Doran and R. A. Burnett, in *Interatomic Potentials and Simulation of Lattice Defects*, eds. P. C. Gehlen, J. R. Beeler, Jr. and R. I. Jaffee, (Plenum Press, NY, 1972) 403.
27. J. B. Sanders, *Rad. Eff.* **51,** 43 (1980).
28. U. Theis and H. Wollenberger, *J. Nucl. Mater.* **88,** 121 (1980).
29. T. H. Blewitt, A. C. Klank, T. Scott, and W. Weber, *Proc. Int. Conf. on Radiation-Induced Voids in Metals*, Albany, NY, 1971, eds J. W. Corbett and L. C. Ianniello, 757 (1972).
30. M. J. Norgett, M. T. Robinson, and I. M. Torrens, *Nucl. Eng. Design*, **33,** 50 (1975).
31. W. Schilling, P. Ehrhart, and K. Sonnenberg, *Proc. Int. Conf. on Fundamental Aspects of Radiation Damage in Metals*, Gatlinburg, TN, Oct, 1975, eds M. T. Robinson and F. W. Young, 470 (1976).
32. R. S. Averback, R. Benedek, and K. L. Merkle, *J. Nucl. Mater.* **75,** 162 (1978).
33. D. G. Doran, R. L. Simons, and W. N. McElroy, in *Properties of Reactor Structural Alloys After Neutron or Particle Irradiation*, ASTM STP 570, 290 (1975).
34. D. G. Doran and J. O. Schiffgens, *Proc. of the Workshop on Correlation of Neutron and Charged Particle Damage*, Oak Ridge, TN, June, 1976, CONF-760673, (1976).
35. J. R. Beeler, Jr., *Phys. Rev.* **150,** 470 (1966).
36. T. Muroga and S. Ishino, *J. Nucl. Mater.* **117,** 36 (1983).
37. T. Muroga, K. Kitajima, and S. Ishino, *J. Nucl. Mater.* **133/134,** 378 (1985).